Journal of Fluids and Structures (2000) **14,** 593–612
doi:10.1006/jfls.2000.0292, available online at http://www.idealibrary.com on IDEAL®

SIMPLE RESISTIVE MODELS FOR STEADY FLOW THROUGH UNIFORM AND TAPERED-STIFFNESS COLLAPSIBLE TUBES

C. D. BERTRAM

Graduate School of Biomedical Engineering, University of New South Wales Sydney, 2052, Australia

(Received 10 March 1999, and in final form 18 January 2000)

An extremely basic model is postulated and examined numerically, to find out which aspects of observed steady-flow collapsible-tube behaviour are predicted and can be explained. The model in simplest form states that the tube has a fixed viscous resistance per unit length when not collapsed, and a higher one when collapsed. Collapse occurs where the falling internal pressure in the streamwise direction causes negative transmural pressure to pass a fixed threshold set by tube wall stiffness. This model suffices to explain (i) the sigmoidal dependence of pressure drop on flow rate when external pressure is fixed, (ii) the weak dependence of pressure-drop on flow rate when downstream transmural pressure is fixed and (iii) the weak dependence of flow rate on pressure drop when upstream transmural pressure is fixed. The effects of incorporating more realistic collapse behaviour (finite compliance once the tube buckles, varying compliance once opposite walls are in contact) on these dependencies are examined. The model is also used to explore the several qualitatively distinct configurations that may be taken up by a tube which varies in stiffness along its length.

1. INTRODUCTION

STEADY FLOW THROUGH COLLAPSIBLE TUBES has been investigated in detail through experimental, theoretical and numerical studies. While sophisticated models are certainly necessary in the quest for quantitative agreement with observed behaviour, they are not necessarily optimal for showing what aspects of a collapsible tube must at minimum be included to model a given behaviour qualitatively. One of the simplest possible models for steady flow through a collapsible tube is the one in which the tube has one resistance per unit length when collapsed, and a lesser one when not (Fry *et al.* 1980). It is of interest to explore how much of collapsible-tube behaviour can be seen in (or explained by) such a simple model.

Already the above model definition implies some further assumptions (or idealizations or simplifications, depending on one's point of view) about the tube behaviour. Most importantly, this statement defines a "tube law", accepted jargon for a purely local relation between transmural pressure and cross-sectional area. While such an assumption underpins many, much more sophisticated models than this one, it is not true; the local tube cross-sectional area is also affected by any differing cross-sectional area in neighbouring cross-sections (Bertram 1987; Elad *et al.* 1992; Heil & Pedley 1996). Secondly, the statement assumes a particular form of that tube law, one in which viscous pressure drop along the tube has no effect on area beyond setting the location of collapse. In reality, flow rate causes an area-dependent pressure drop, which changes the transmural pressure and hence diminishes the area along the tube. In short, resistance to flow is not constant along the

0889–9746/00/070593 + 20 $35.00/0

tube, whether it is collapsed or not (the latter state will henceforth be referred to as open), and versions of the model will be presented in which this assumption is relaxed for the collapsed state. Thirdly, it is of course unrealistic to assume an abrupt (discontinuous) change in area and resistance at any matching point along the tube where collapse begins or ends. Consequences of relaxing this assumption have also been explored and will be touched on briefly below. But for now all such considerations will be regarded as of secondary importance; they can modify behaviour extensively, but do not change the broad outlines sought here. The ideas developed herein are an extension of a model used by Bertram (1995).

The arrangement of the paper is unconventional, in that it is more sensible to present the results from each variant of the model in close association with the description of the model itself; thus, rather than separate methods and results, the next two sections of the paper present first uniform-tube models, then tapered-stiffness models. The results are discussed in Section 4, and the conclusions are brought together in Section 5.

2. UNIFORM TUBES

2.1. The Basic Model

It will be assumed that all pressures are relative to that at the exit from the system, i.e. the downstream end of whatever apparatus lies downstream of the collapsible tube. The simplest situation experimentally is then to vary the upstream head p_u and/or the pressure external to the tube, p_e. Beyond the tube itself, the model comprises a resistance per unit length in the upstream and downstream systems which is equal to that in the collapsible tube when it is open. This is equivalent to assuming that the up- and downstream systems consist of rigid tubing having the same diameter as the open collapsible tube. Collapsible tube length is normalized to 1, such that $x/L = 0$ at the upstream end and $x/L = 1$ at the downstream end. The rigid pipes have length L_u upstream and L_d downstream, where $L_u = L_d = 2$ initially. In the most basic version of the model, the pressure drop Δp is given by

$$\Delta p = R \Delta x Q,$$

where Δx is the distance along the tube or the rigid pipe beyond it, Q the volume flow rate, and the resistance per unit length, R, takes the value R_c or R_n depending on whether the tube is collapsed or not. The tube is assumed to collapse when the internal pressure $p(x) < p_c$ locally, where $p_c = p_e - \Delta p_c$ for a uniform tube, p_e is the (uniform) pressure external to the tube, and Δp_c, a property of the tube, is the magnitude of the negative transmural pressure needed to cause collapse, i.e. $p_c < p_e$. The above formulation, with $R = R_c$ or R_n, is equivalent to the most basic tube law considered, which allows just two values: $A = 1$ when $p \geq p_c$ and $A = A_c$ when $p < p_c$; $A_c = 0{\cdot}2$ (Shapiro 1977; Bertram 1987). Pressure drop is then

$$\Delta p = \frac{k}{A^2} \Delta x Q,$$

where $k = 1{\cdot}5$ arbitrarily. A more exact model would have $k = k(A)$, converting the constant to a shape factor accounting for the greater viscous resistance offered by noncircular cross-sections. Note that $R_c/R_n = 1/A_c^2$; the resistance ratio thus takes the value 25, although the findings of this paper, which are qualitative, do not depend on particular values. Parameter values for all the various versions of the model considered in this paper are gathered together in Table 1.

TABLE 1

Parameter settings for each of the situations considered. A blank indicates either that the parameter did not exist in the version of the model in use, or that its value varied

Fig.	L_u	L_d	A_c	A_p	n	R_c/R_n	k	p_{c1}	$p_c - p_2$	$p_c - p_1$	$\mathrm{d}\Delta p_c/\mathrm{d}x$
1	2	2	0·2	—	—	—	1·5	45	—	—	—
2	2	2	0·2	—	—	—	1·5	—	45	—	—
3	2	2	0·2	—	—	—	1·5	—	—	−3	—
4	2	2	0·2	0·003	—	—	1·5	—	—	−3	—
5	2	2	0·25	0·075	4	—	1·5	—	—	−3	—
8	0	1	—	—	—	4	1·5	0·2	—	—	−0·6
9	0	1	—	—	—	4	1·5	0·6	—	—	0·2
10	0	1	—	—	—	4	1·5	1·5	—	—	1·4
11a	0·5	0·5	—	—	—	3	1·5	0·9	—	—	0·9
11b	0·5	0·5	—	—	—	3	1·5	1·1	—	—	0·9
11c	0·5	0·5	—	—	—	3	1·5	1·3	—	—	0·9
11d	0·5	0·5	—	—	—	3	1·5	1	—	—	0·8
11e	0·5	0·5	—	—	—	3	1·5	1·1	—	—	0·8
11f	0·5	0·5	—	—	—	3	1·5	1·2	—	—	0·8
11g	0·5	0·5	—	—	—	3	1·5	1·3	—	—	0·8
12a	0	1	—	—	—	4	1·5	0·7	—	—	−0·3
12b	0	1	—	—	—	4	1·5	0·8	—	—	0
12c	0	1	—	—	—	4	1·5	0·9	—	—	0·2
12d	0	1	—	—	—	4	1·5	1	—	—	0·4
12e	0	1	—	—	—	4	1·5	1·6	—	—	1·6

Figure 1(a) shows how the pressure in the tube itself varies for a series of different flow rates (in dimensionless and arbitrary units), from 0·5 to 6·0 in steps of 0·5. The model of course also yields $p(x)$ in the rigid pipes, from a maximum of p_u at the upstream end of the whole system to zero at the downstream end, but the figure concentrates on just the collapsible segment. As flow rate increases so must p_u, but not in proportion. Each of the curves with a slope discontinuity shows the tube open from the upstream end and collapsed from the point along the tube where the slope changes. The tube collapses at the point where p falls below the fixed value p_c (here, 45). The tube is collapsed along its whole length at the two lowest flow rates. Figure 1(b) shows for each flow rate the difference between the internal pressures at the entrance and the exit of the tube, i.e. the left- and right-hand sides of Figure 1(a). This is $p_1 - p_2$, the pressure drop along the tube. Conrad (1969) and others have shown that this pressure drop increases steeply at low flow rates (region III), then decreases again at higher flow rates (thereby defining a region II of usually negative incremental resistance) then increases again, but with much shallower slope, when the tube is fully open at the highest flow rates (region I). Figure 1(b) does not extend as far as region I, but does display regions II and III.

The model also makes clear that the negative slope of region II is not an innate tube property, but depends on factors external to the tube. The negative slope is a reflection of the fact that the variation of p_2 with Q is greater than that of p_1 when the tube collapses along its length. However, the increase of p_2 with Q is a function purely of the resistance provided downstream of the tube. In the case shown, the up- and downstream systems were given a length equal to twice the length of the tube itself. If the downstream length is made the same as the tube length, the descending limb of the curve becomes approximately flat, and if it is made shorter than the tube, becomes a second positive limb of reduced slope. This has implications for the use of the negative slope to predict instability (Conrad 1969).

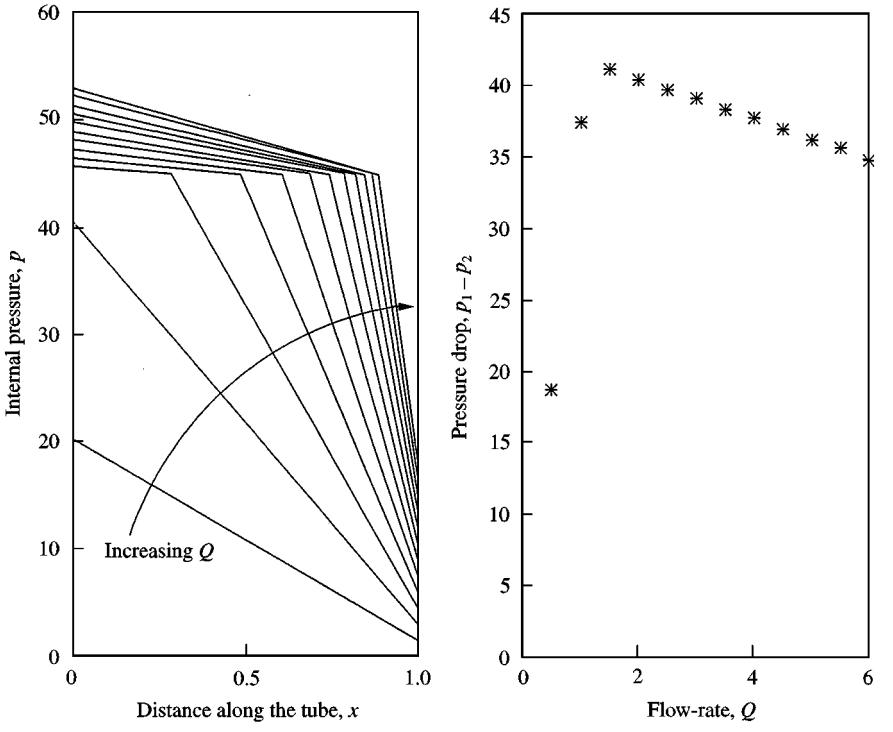

Figure 1. (a) Curves of internal pressure variation along the length of a collapsible tube having only two states: open or collapsed, each providing a fixed resistance per unit length to flow. Each curve is for a different value of the flow rate. (b) The pressure drop along the whole collapsible tube is plotted against flow rate.

Conrad [private communication; Discussion (1995) of Yamane & Orita (1994)] has suggested that the appropriate criterion involves instead the negative slope of the relation of flow rate to pressure drop over that section of the tube which is collapsed. In the present context, this pressure drop is $p_c - p_2$. However, the negative slope of $\mathrm{d}(p_c - p_2)/\mathrm{d}Q$ in region II is still a function of the rigid tube length or other resistance downstream. This dependence on factors external to the tube itself is a well-known drawback of presenting pressure drop as a function of flow rate at constant external pressure.

2.2. Pressure-Drop and Flow Rate Limitation

This simplest collapsible-tube model can also be used to demonstrate pressure-drop limitation and flow rate limitation. These behaviours are innate to the tube; they do not depend on external factors. Pressure-drop limitation occurs when the transmural pressure at the downstream end of the tube is held constant. An example is shown as Figure 2. The collapse pressure now varies with the pressure at the downstream end, such that $p_c - p_2 = 45$ (arbitrary units). All other parameters being unchanged from Figure 1, the curve of $p_1 - p_2$ now shows a steep section III (collapse all the way along the tube), and a more gently sloped section II, where the pressure drop is relatively independent of the flow rate. Unlike the corresponding curve in Figure 1(b), this one is independent of the length of the external rigid-tube sections, and thus reflects purely the properties of the collapsible tube.

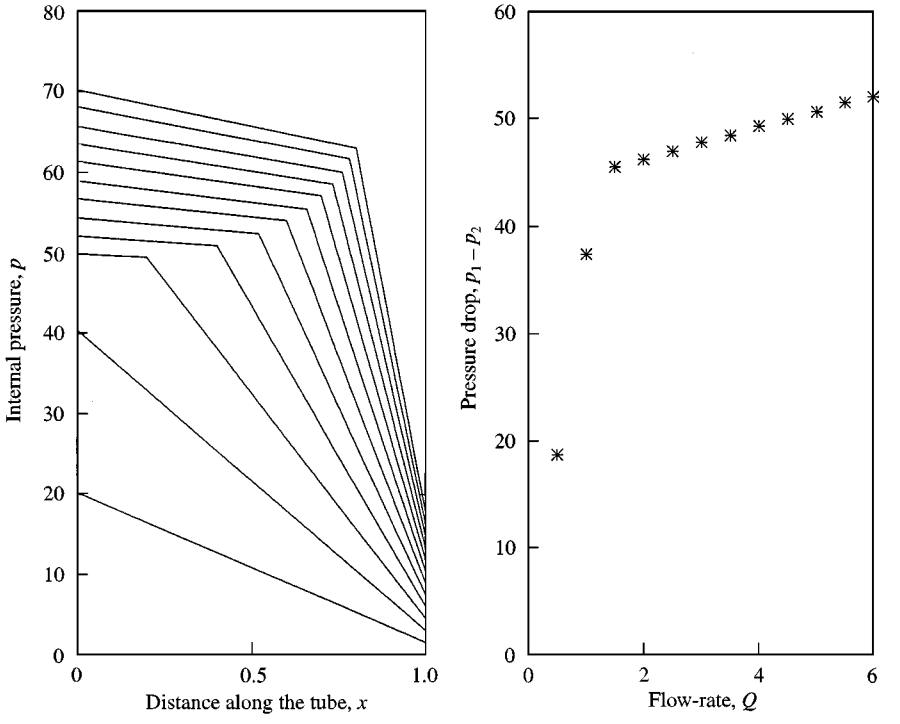

Figure 2. (a) Variation of pressure along the tube when downstream transmural pressure $p_e - p_2$ is constant, and therefore $p_c - p_2$ is constant. (b) Pressure drop versus flow rate, showing pressure-drop limitation.

Flow-rate limitation occurs when the transmural pressure at the upstream end is held constant. This situation is substantially more difficult to solve; it is no longer appropriate to take a series of flow rate values as inputs, and instead a series of values of p_u (from 10 to 70 in steps of 4) was prescribed. The unknowns are then the flow rate, the collapse pressure and the collapse position. Figure 3 shows results for $p_c - p_1 = -3$; again the external length is twice that of the collapsible tube, both upstream and downstream. The pressure drop $p_1 - p_2$ now increases initially slowly (tube open along the whole length) then the slope increases such that $\mathrm{d}(p_1 - p_2)/\mathrm{d}Q$ is greater than $(p_1 - p_2)/Q$. This defines flow rate limitation; the flow rate is now only weakly dependent on the pressure drop. Again, as for Figure 2, the pressure-drop/flow rate relation is independent of the downstream resistance as represented by the length of the rigid pipe beyond the tube, although since the calculation here starts from a value of p_u, the location of the points along the relation varies with L_d.

2.3. Negative Effort Dependence

Such flow rate limitation is of physiological interest because it occurs in various body conduits, including the small airways of the lung, the urethra, and the veins returning blood to the thoracic venae cavae. In some *in vivo* situations, and also in collapsible tubes on the bench, the flow rate is rather more independent of the pressure drop than is the case in Figure 3, and often even displays "negative effort dependence", a term from lung-function testing meaning that the flow rate decreases as the pressure drop increases. What added features are needed in a model which can imitate this behaviour? This question was in fact

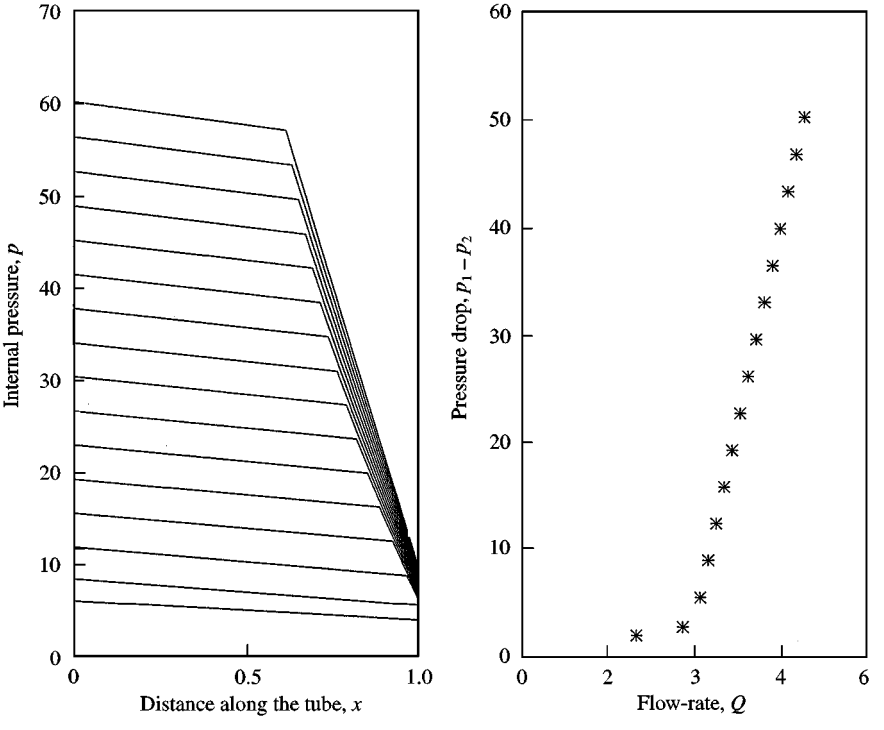

Figure 3. (a) Variation of pressure along the tube when upstream transmural pressure $p_e - p_1$ is constant, and therefore $p_c - p_1$ is constant. Parameters otherwise as in Figure 1, except that instead of specifying a series of Q values, a series of p_u values is solved. Note that under these conditions it is the *lowest* two values of head which produce no collapse anywhere along the tube. (b) Pressure drop versus flow rate, showing flow rate limitation.

the original motivation behind the series of small computer models on which this paper reports. Figure 4 shows flow limitation when the pressure–area relation is made one step more realistic, by allowing the cross-sectional area to decrease with negative transmural pressure after collapse. The tube law was modified for $p < p_c$ to

$$A = A_c - A_p(p_c - p);$$

the value of $A_p(= 0{\cdot}003)$ describes the compliance of the tube once collapsed. Whereas up to now the collapsed area was always 0·2, now it decreases linearly below 0·2 with a slope $\mathrm{d}A/\mathrm{d}p = 0{\cdot}003$ [Figure 4(a)]. [In the process, the model has acquired more of the characteristics of a distributed model. Although previously the pressure was defined at all points along the tube, it was simply a straight line joining lumped pressures at the ends which could be evaluated without consideration of the interior of the tube other than the location of collapse. Now the flow rate is found from the specified p_u by solving a problem involving integration of the pressure gradient along the tube. Of course, the model is still confined to steady flows, and has no concept of time-dependent distributed phenomena such as wave travel.] The resulting curves of internal pressure versus position along the tube, including the upstream and downstream sections external to the collapsible segment, are shown in Figure 4(b), and the relation between $p_1 - p_2$ and Q in Figure 4(c). Comparison with Figure 3(b) shows that while the relation is little altered at lower $p_1 - p_2$ values, it becomes progressively steeper; by $p_1 - p_2 = 50$, Q is only 2·6, where previously it had reached 3·2.

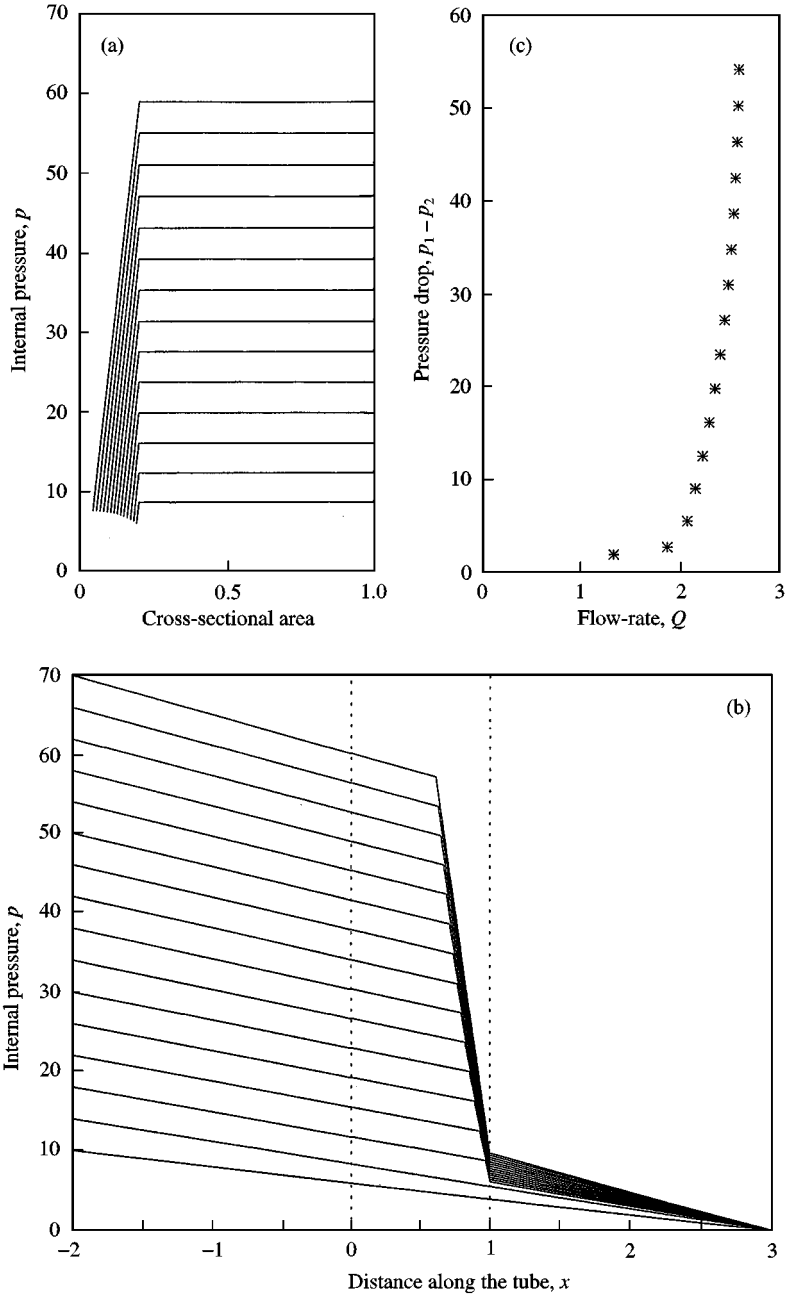

Figure 4. As Figure 3, but with a fixed nonzero compliance once collapsed, allowing the tube resistance per unit length to increase with further reduction in internal pressure, causing the internal pressure to decline progressively faster along the tube after the collapse point. (a) Internal pressure along the collapsible tube itself versus area, for each of the 16 p_u-values solved. Only 14 curves are visible, because in two cases the tube did not collapse ($A = 1$). (b) Internal pressure versus position along the tube and in the rigid pipes. (c) Pressure drop versus flow rate, showing improved flow rate limitation relative to Figure 3. The pressure drop is the difference between $p(x)$ as in (b) at $x = 0$ and at $x = 1$.

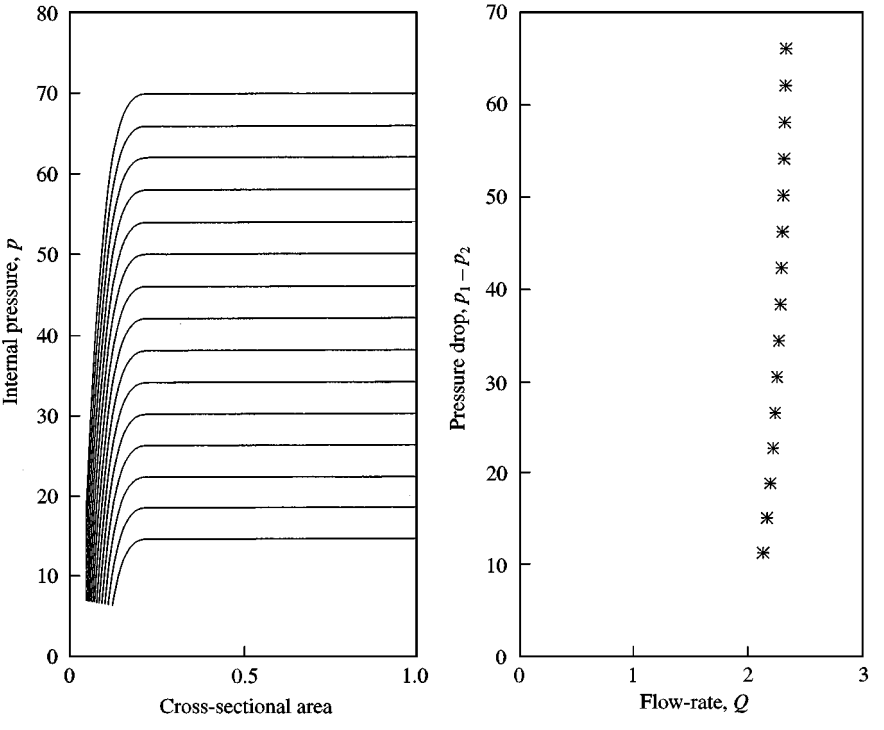

Figure 5. As Figure 3, but with a progressively reducing nonzero compliance once collapsed. (a) Curves of internal pressure against area. (b) Even more complete flow rate limitation is the result, but flow rate still always increases with pressure drop; negative effort dependence is absent.

This modified pressure–area relation is of course still unrealistic even in the region where collapsed compliance is now permitted, in that sufficient negative transmural pressure will produce negative areas. In reality, collapsed tubes become stiffer as their area reduces. For Figure 5, the tube law was therefore further modified for $p < p_c$ to

$$A = A_c - A_p(p_c - p)^{1/n},$$

where $A_c = 0{\cdot}25$, $A_p = 0{\cdot}075$, and $n = 4$. Figure 5(a) shows the form of the resulting tube law. Figure 5(b) shows that the effect on the flow limitation is to steepen the progressively steeper part of the curve; still less flow rate is produced for a given high value of pressure drop along the tube.

However, there is no sign of negative effort dependence in any of Figures 3–5. Nor is it produced by introduction of finite compliance for the tube between first buckling and first opposite-wall contact (not shown), thereby avoiding a discontinuity in area along the tube. Figure 6 shows sketches of what must transpire for negative effort dependence to occur, based on ideas of Mead *et al.* (1967). Recall that as pressure drop increases from zero, the flow rate must start from zero, rise to a peak, then fall back to a level that it has previously passed through. Figure 6(a) shows the expected situation when the flow rate first attains that level, here called $Q_{\min}$; the internal pressure has descended to the level p_c at the downstream end of the collapsible tube, i.e. $p_2 = p_c$, where for flow rate limitation p_c is a fixed level below p_1. Turning to Figure 6(b), p_1 and p_e have been increased in concert, and of course Δp_c is always fixed by the tube properties. The flow rate has increased in Figure 6(b) beyond its value in Figure 6(a), as indicated by the steeper slope of the pressure-drop profile in the rigid pipe section beyond $x = L$ and in the noncollapsed part of the tube starting at $x = 0$; this

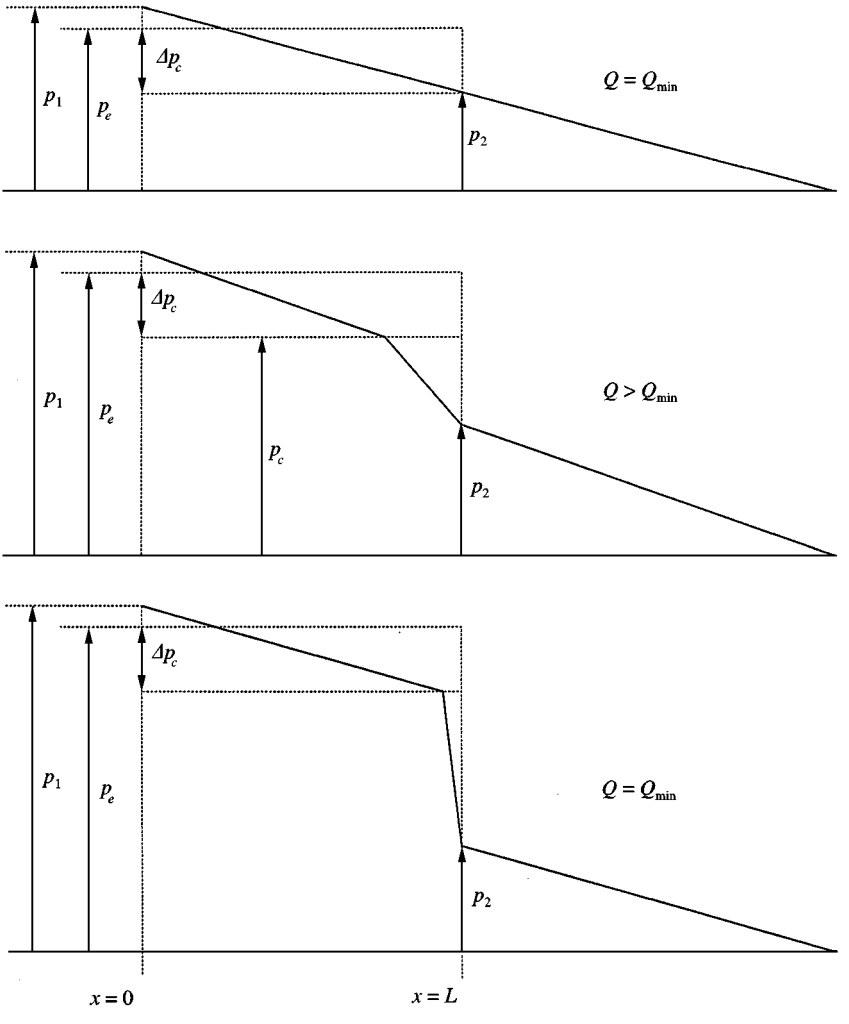

Figure 6. Sketches of negative effort dependence as manifested in a collapsed tube, after Mead *et al.* (1967): (a) when flow rate first reaches the eventual limit; (b) at or close to the peak flow rate; (c) at the limiting flow rate.

situation prevails at and around the peak flow rate. If, with still further increase in p_1 and p_e, the flow rate is then to sink back to approximately that shown in Figure 6(a), p_2 must fall back to its value in that sketch, and the pressure-drop profile must revert to that slope everywhere except in a very short collapsed section of tube at the downstream end. Figure 6(c) shows the final state; whereas at the flow rate peak a substantial part of the downstream end of the tube was collapsed, the high p_1 and predetermined flow rate now ensure that collapse must be limited to a small downstream segment, across which there is a very large pressure drop, implying a high degree of collapse. In fact the flow rate and p_2 are still slightly greater than in Figure 6(a); were this not so, the pressure in the tube would only descend to p_c at exactly $x = L$, and a finite drop in pressure from p_c to p_2 would have to occur in zero collapsed-tube length, implying an unrealistic infinite viscous resistance in the collapsed section. Thus, after the peak flow rate has been passed, Q_{min} takes on the aspect of a never-again-attained asymptote. Although these sketches are drawn with

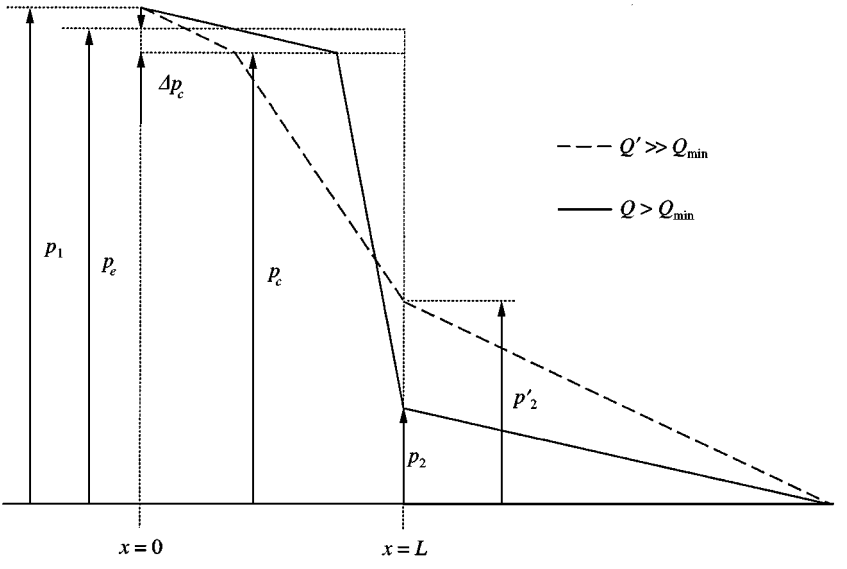

Figure 7. A possible explanation of what determines how much peak flow rate exceeds the flow-limited flow rate. Pressure-drop profiles are shown for two different tubes, one of which changes its resistance much more when it collapses than the other. A small ratio of resistances leads to a large degree of peak flow rate excess over the flow rate limit.

straight lines, implying the simplest two-fixed-resistances model, Figure 6(c) in fact forces abandonment of the assumption that collapsed resistance per unit length is a fixed multiple of open-tube resistance. It can be concluded that a more realistic tube law as shown in Figure 5(a) is definitely necessary to the production of negative effort dependence; however, on the basis of the outcome shown in Figure 5(b) it is not a sufficient condition.

The model with two fixed values of resistance per unit length can however be used to provide a partial answer to the question: what might determine how much the peak flow rate of Figure 6(b) exceeds the final flow rate of Figure 6(c)? Figure 7 shows sketches of the variation of pressure along the tube as a function of position again, for two different ratios of collapsed-tube resistance per unit length to open-tube resistance. As in Figure 6, the ratio corresponds to the ratio of the slope of the pressure-drop profile when collapsed to that when open. Both profiles are assumed to correspond to the position in Figure 6(b), where the flow rate is near or at its peak. The same values of p_1 and p_c are used in both cases, but the peak flow rate (and p_2) is much greater in the case where the collapsed tube increases its resistance over the open tube by only a small factor; a large factor leads to a smaller peak flow rate. Note again, however, that this diagrammatic construction assumes that the peak flow rate is attained in the two tubes at the same value of p_1; there is no necessary reason why this should be so, and in fact in the absence of a specified pressure–area relation the argument does not determine the value of p_1 at peak flow rate. Furthermore, despite the fact that the two tubes have been assumed to behave so differently in terms of how much resistance per unit length is augmented upon collapse, the same value of Δp_c is assumed for both. These are somewhat incompatible assumptions, so this use of the model must be viewed with caution.

Finally, it should be noted that the failure of the present model to predict negative effort dependence does not mean that viscous flow limitation as opposed to wavespeed flow limitation (Griffiths 1975; Wilson *et al.* 1986) is inherently unable to produce this effect.

Hayashi *et al.* (1994) and Jensen (1998) have proved with rather more elaborate models of viscous flow limitation than that examined here that negative effort dependence can be produced through this mechanism.

3. TAPERED-STIFFNESS TUBES

3.1. Possible Collapse Configurations

Recently, there has been revived interest in the properties and behaviour of collapsed tubes with tapering wall stiffness along their length (Kamm *et al.* 1991, 1993; Ohba *et al.* 1998; Bertram & Chen 2000), first mooted by Shapiro (1977). Such tubes can be simply modelled by letting p_c vary with distance along the tube, so that $p_c(x) = p_e - \Delta p_c(x)$, implying a constant p_e but a varying transmural pressure required to bring about collapse at different points. In this paper, a linear variation of tube stiffness was assumed, such that

$$\Delta p_c(x) = \Delta p_{c1} + (\Delta p_{c2} - \Delta p_{c1}) \frac{x}{L}.$$

The case where p_c increases with distance in the stream-wise direction, corresponding to decreasing stiffness downstream, is relatively trivial; as in a uniform tube, there are still just three possibilities: collapse along the whole length, collapse nowhere, or collapse from an intermediate position as far as the downstream end. Figure 8 illustrates these behaviours. For purposes of illustration, this model dispenses with pressure drop in the rigid section upstream of the collapsible tube, i.e. $L_u = 0$, and the resistance per unit length when collapsed is assumed to be four times that when the tube is open, i.e. $R_c/R_n = 4$. Flow rates from 0·05 incrementing by 0·05 up to 0·9 are shown.

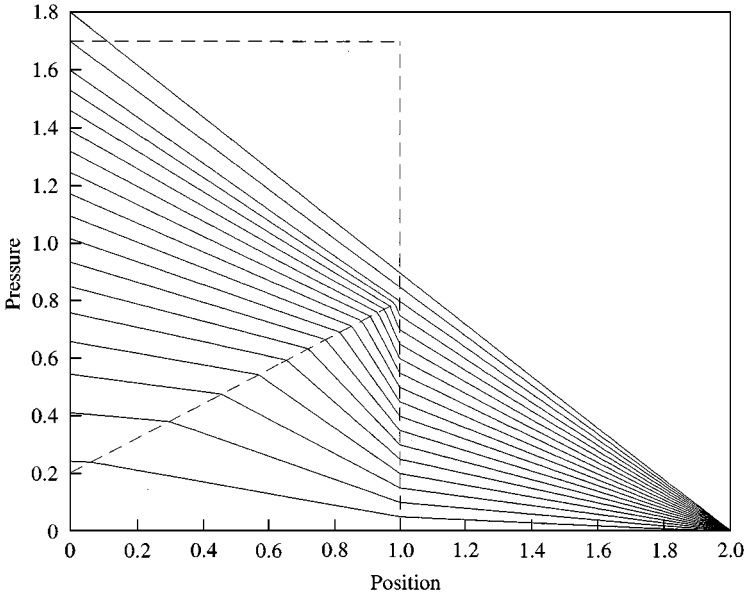

Figure 8. Pressure-drop profiles for a tapered-stiffness tube arranged with its stiff end upstream. The effect is not qualitatively different from the case of a uniform tube. The horizontal dashed line shows a putative value of $p_e = 1{\cdot}7$, but the tube configuration depends only on the sloping line of p_c gained by subtracting the local transmural pressure magnitude required for collapse (Δp_c) from p_e. Because of the taper, Δp_c decreases with distance along the tube.

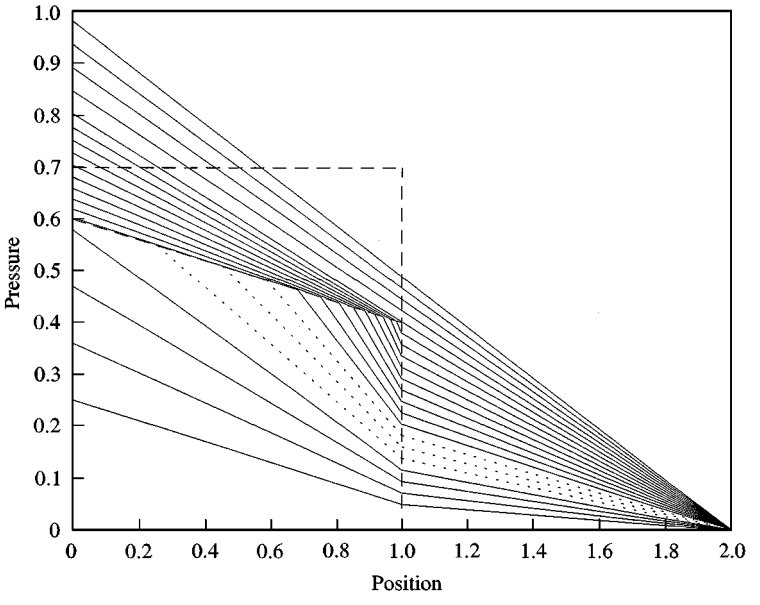

Figure 9. Pressure-drop profiles for a tapered-stiffness tube arranged with its stiff end downstream, in which the rate of stiffness variation is insufficient to offset the viscous pressure drop along the tube even when the tube is open. Although the tube still can only display collapse from an intermediate point to the far end, as in a uniform tube, a new feature is that certain flow rates (corresponding to pressure profiles in dotted lines) cannot be produced by adjustment of the pressure at the upstream end of the collapsible segment. Parameters as for Figure 8, except for p_e and $\Delta p_c(x)$ which are readily discerned from the Figure; Q from 0·05, increasing by steps of 0·022 to 0·5.

Rather more varied possibilities occur when the taper is such that the tube gets stiffer downstream. A functional definition of a tapered-stiffness tube may be based on the condition that the rate of stiffness increase is sufficient that p_c decreases faster than the pressure in the open tube, i.e.

$$\frac{\mathrm{d}\Delta p_c}{\mathrm{d}x} > -\frac{\mathrm{d}p}{\mathrm{d}x}.$$

Figure 9 shows what happens when this condition is *not* met (for the case where the upstream length is zero, i.e. p_1 is also the flow-driving head). As in a uniform tube, if collapsed at all, the tube always collapses up to the downstream end. However, a noteworthy difference from uniform-tube behaviour is that there is a range of unattainable flow rates, indicated by the three pressure profiles shown by dashed lines. To see how this arises, consider the case of the lowest flow rate above the excluded ones. This flow rate causes the pressure along the open part of the tube to decrease scarcely more rapidly than p_c; the profile and the p_c line are almost parallel. Starting from zero pressure at the system exit, the construction for the next lower flow rate in this incremental series would present no problem until the point where the steep profile in the downstream collapsed tube part met the sloping p_c line. But crossing that line would cause the profile to revert to a slope which would bring it back below p_c, suggesting a p_1 value corresponding to collapse all the way along the tube and a lower flow rate altogether. Two different solutions to this dilemma exist. If indeed flow rate was the controlled variable in the putative corresponding experiment, the result would be that $p_1 = p_c$ at the upstream end ($x/L = 0$) and the profile would

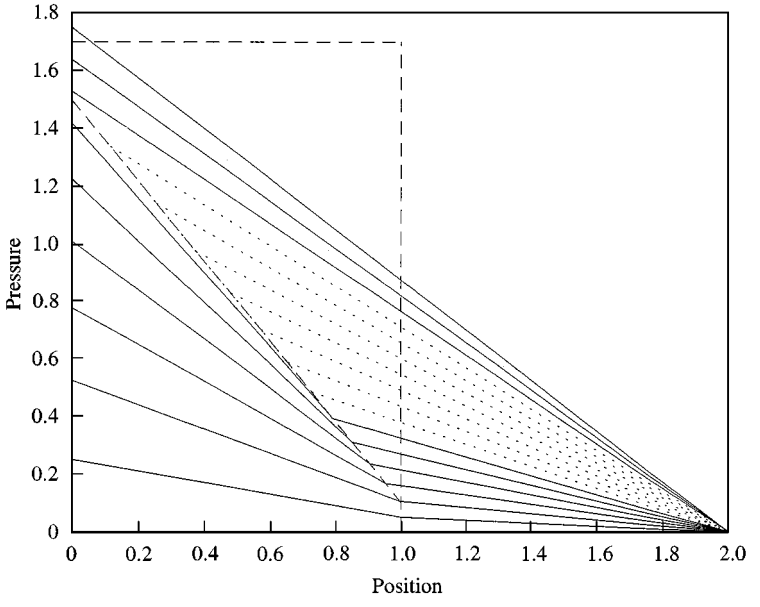

Figure 10. When the rate of streamwise stiffness increase exceeds the rate of viscous pressure drop for the open tube, the tapered-stiffness tube can exhibit collapse from the upstream end as far as an intermediate point along the tube. All parameters other than $\Delta p_c(x)$ as in Figure 8; Q from 0·05, increasing by steps of 0·055 to 0·9.

follow the p_c slope until collapse proper occurred at the appropriate intermediate point along the tube. However, in practice, flow rate has never yet been the controlled variable in a collapsible-tube experiment. If the upstream pressure was controlled, as is usual experimentally, then a jump in flow rate across the dashed-line range would be observed.

A similar band of excluded flow rates occurs if the stiffness taper is such that p_c decreases more quickly than the pressure in the collapsed tube, as shown in Figure 10. In this case, there are seven profiles that could only be observed in a hypothetical controlled-flow rate experiment. This plot shows the defining characteristic of a tapered-stiffness tube, that collapse can cease at some intermediate point, having started at the upstream end; such a tube only collapses as far as the downstream end if collapsed everywhere. Of course, this functional definition means that whether a given tube behaves as tapered depends on the resistance (here, rigid-tube length) downstream, and also on p_e; as p_e is varied, the whole sloping line for p_c moves vertically, intersecting open-tube pressure-drop lines of greater or lesser slope.

What happens if the rate of pressure drop just equals the rate of p_c decrease? This apparently unlikely coincidence in fact occurs over substantial ranges of parameter space in the model, because of the assumption that there is a fixed ratio of collapsed- to open-tube resistance. As a result of this, the tube internal pressure is forced to track the p_c line until it can break away at an appropriate slope that reconciles the boundary conditions, as occurred in Figures 9 and 10. Figure 11 illustrates this behaviour in the context of the usual experimental situation, where p_u is set then p_e is varied, and the flow rate finds its own level. Resistance per unit length when collapsed is here assumed to be three times that when the tube is open. Figure 11(a–c) shows pressure-drop profiles for a tapered-stiffness tube at three different levels of p_e, increasing from (a) to (c), leading to three different lines of p_c. Each pressure profile corresponds to one $p_c(x)$-line. At the lowest p_e, the tube never collapses; at the highest, it is collapsed all the way along. At the intermediate p_e level, the problem of

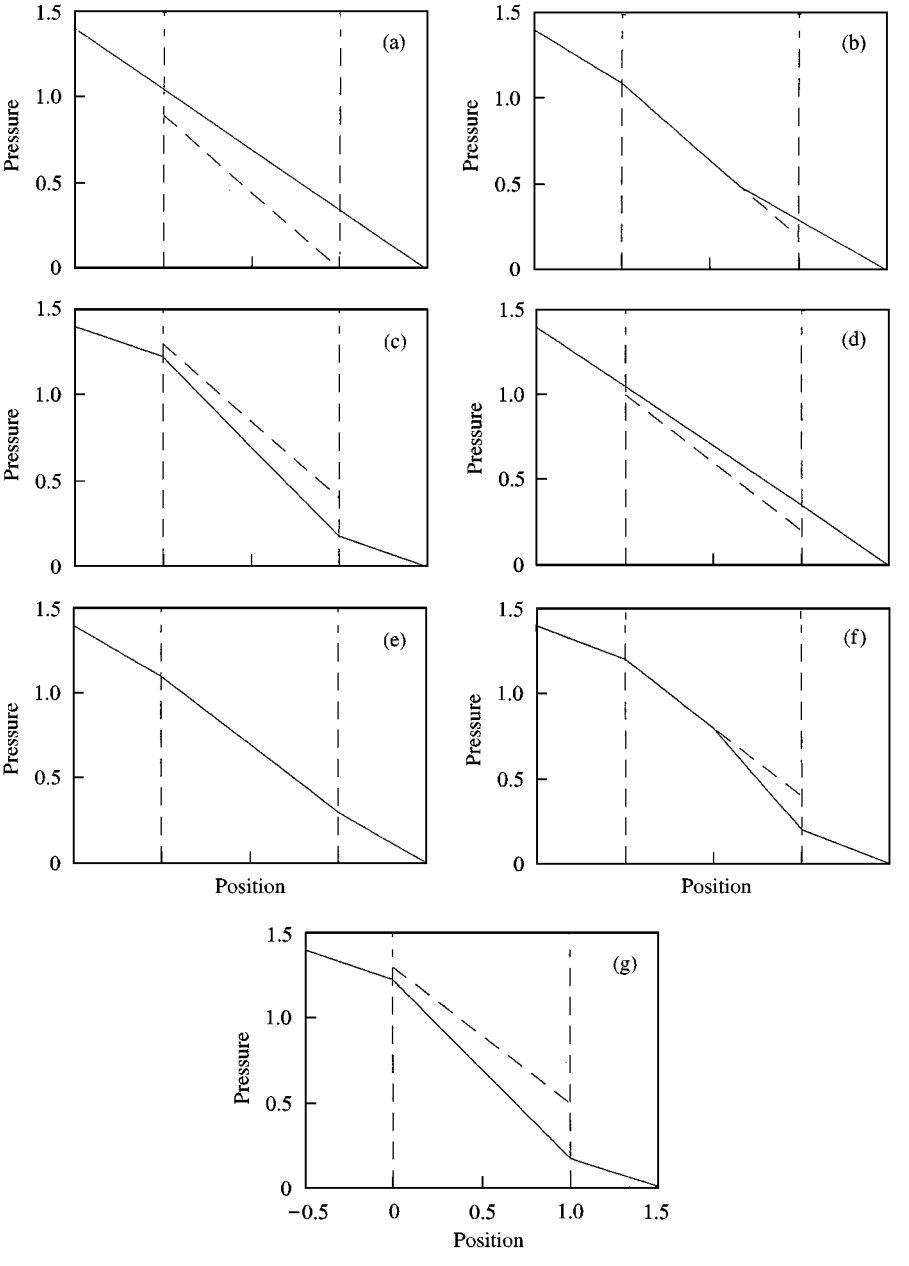

Figure 11. Internal pressure $p(x)$ along tapered-stiffness tubes, when upstream head is constant (here, $p_u = 1{\cdot}4$) and external pressure is raised (see Table 1). The sloping broken line in each panel shows $p_e(x)$. Panels (a–c) show one tube, with $\mathrm{d}\Delta p_c/\mathrm{d}x = 0{\cdot}9$; panels (d–g) show another, with $\mathrm{d}\Delta p_c/\mathrm{d}x = 0{\cdot}8$ (slightly less stiffness taper). Panels (a)–(c), for three successively greater values of external pressure, show (a) no collapse, (b) an internal pressure-drop which exactly tracks the rate of stiffness change down the tube, as far as the point where the tube reopens fully, and (c) collapse of the whole tube. The resulting flow rate, which corresponds to the slope of $p(x)$ upstream or downstream of the collapsible tube ($x/L < 0$ or $x/L > 1$), was $Q = 0{\cdot}7$, $0{\cdot}6$ and $0{\cdot}35$ for (a), (b) and (c), respectively. With less taper, panels (d)–(g), for four successively greater values of external pressure, show (d) no collapse, (e) tracking as in (b) but now all the way along the tube, (f) tracking as far as where full collapse takes over, and (g) collapse of the whole tube. The resulting flow rate was $Q = 0{\cdot}7$, $0{\cdot}6$, $0{\cdot}4$ and $0{\cdot}35$ for (d), (e), (f) and (g), respectively.

reconciling the boundary constraints of p_u at the driving end and zero at the drain end is solved by the tube tracking the p_c line as far as the point where reverting to the open-tube configuration will meet zero pressure at the downstream end of the system. Note that, whereas the instances of such tracking shown in Figure 10 were impossible experimentally, short of arranging for flow rate control, here tracking occurs under readily obtainable conditions, except insofar as it depends on a fixed resistance ratio.

Tracking can also, as in Figure 9, be followed by full collapse. Figure 11(d–g) shows four p_e values, increasing from (d) to (g) for another tube, with a slightly smaller rate of stiffness taper. The extreme two p_e values [panels (d) and (g)] lead to no collapse and collapse all along as before. The second lowest [panel (e), with the second-lowest sloping broken p_c line] happens to be the case where tracking occurs all the way along the tube; this is indeed a coincidence of parameter values which is not generic. The second highest [panel (f)] shows p_c-line tracking followed by full collapse as far as the downstream end of the tube.

Altogether then, for a tapered-stiffness tube there are six possibilities:

(i) never collapsed,
(ii) collapsed all the way along,
(iii) collapsed as far as an intermediate point,
(iv) collapsed from an intermediate point to the end,
(v) the pressure drop follows the p_c-line until full collapse,
(vi) the pressure drop follows the p_c-line until the tube opens.

3.2. Pressure-Drop versus Flow Rate

Figure 12 shows how taper affects the relation between pressure-drop and flow rate, under conditions of prescribed flow rate as in Figures 8–10. Resistance per unit length when the tube is collapsed is here four times that when open. Panel 12(b) shows the pressure-drop/flow rate relation in the absence of taper; the usual regions I–III are visible. As noted above, region II can be of positive slope when the downstream resistance is small, and this tendency is reinforced here, relative to the case shown in Figure 1, by the use of a smaller ratio (4, as opposed to 25) of collapsed to open resistance. Panel 12(a) deals with a tube of the same average stiffness along its length, but which is tapered so as to become thinner downstream. The effect of the taper is to round the transition between regions II and III, and because the maximum stiffness (at the downstream end) is greater, to move the transition from region II to region I to a higher flow rate. The slope of region I is unchanged from that of the uniform tube [panel 12(b)]; it is region II which has been elevated. Panel 12(c) shows the result of introducing mild stiffness taper in the functionally important direction (stiffer downstream). As yet the taper is insufficient for the tube to satisfy the functional definition above a tapered-stiffness tube; consequently, the pressure profiles are qualitatively unchanged from the uniform tube case shown immediately above. However, the relation between $p_1 - p_2$ and Q no longer exhibits a constant slope in region II, which now takes over from region I at a lower flow rate and gives way to region III at a higher flow rate than in the uniform tube. At no point does the region-II gradient attain the value it had in the uniform tube, and as region III is approached it becomes negative. When the stiffness taper is increased [panel 12(d)], these trends become accentuated. Region II now splits into two distinct sub-regions, one (here, of approximately zero slope) corresponding to the region-II behaviour in panel 12(c), and the other, of negative slope, corresponding to those flow rates where p_c-line tracking is followed by full collapse. Still greater stiffness taper [panel 12(e)] creates a situation where the whole of region II results from p_c-line tracking followed by tube re-opening. As with the tracking in panel 12(d), the region-II slope is then

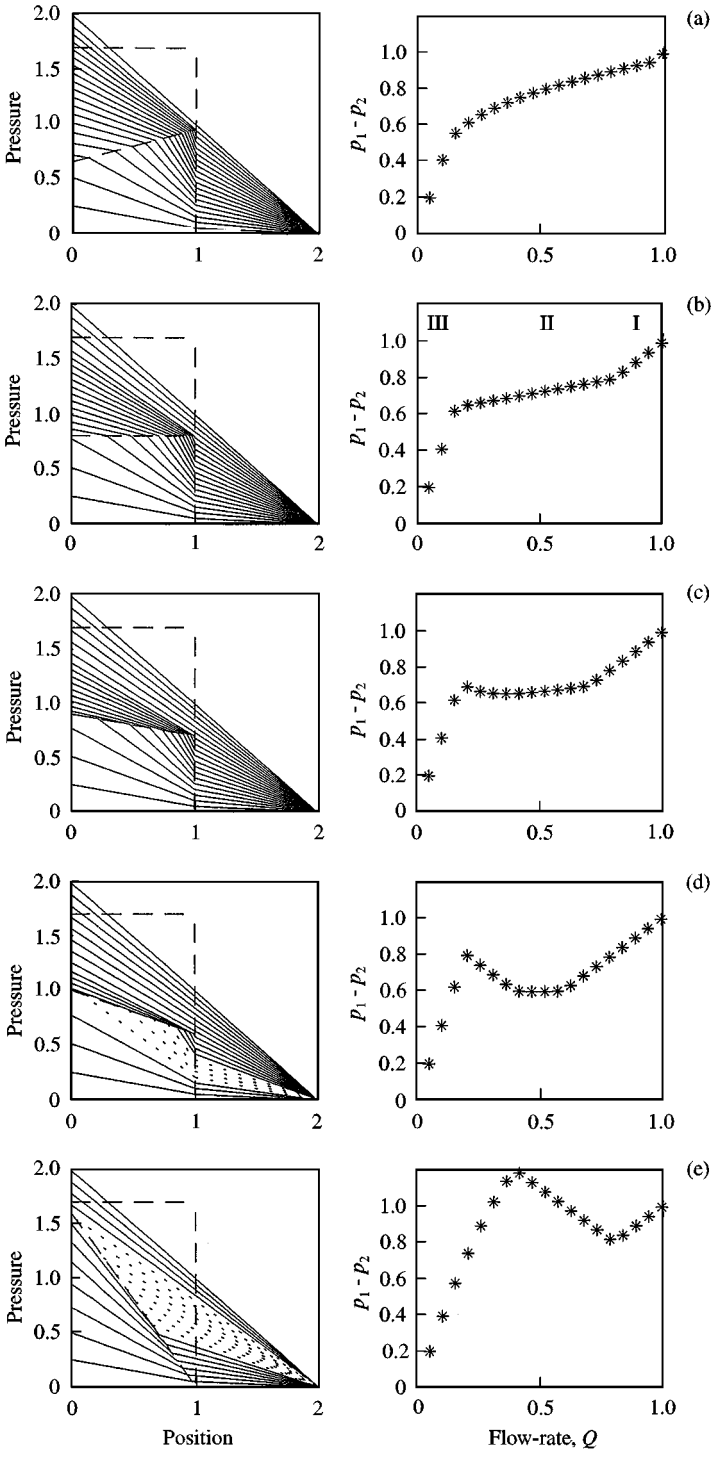

Figure 12. Effects of tube stiffness taper on the relation between pressure drop and flow rate, for prescribed flow rates (Q from 0·05, increasing by steps of 0·0525 to 0·995). p_e is fixed at 1·7, and the average Δp_c along the length of the tube is fixed at 0·9; for the five cases shown, from top to bottom, (a) reverse taper—thinner downstream ($\Delta p_{c1} = 1{\cdot}05$, $\Delta p_{c2} = 0{\cdot}75$), (b) no taper ($\Delta p_c = 0{\cdot}9$), (c) slight forward taper—thicker downstream ($\Delta p_{c1} = 0{\cdot}8$, $\Delta p_{c2} = 1{\cdot}0$), (d) increased forward taper with tracking followed by collapse ($\Delta p_{c1} = 0{\cdot}7$, $\Delta p_{c2} = 1{\cdot}1$), (e) yet more forward taper with tracking followed by reopening ($\Delta p_{c1} = 0{\cdot}1$, $\Delta p_{c2} = 1{\cdot}7$). Regions I–III of the pressure drop/flow rate relation as referred to in the text are indicated on panel (b).

necessarily negative, because p_1 is constant while p_2 increases with flow rate. The intersection with region III occurs at a relatively high flow rate, because reopening at points short of the downstream end of the tube causes a steadily diminishing region-III slope.

Finally, what is the effect of taper on the pressure-drop/flow rate relation under conditions for flow rate limitation? Can taper provide the missing ingredient needed to explain negative effort dependence? Since real tubes display negative effort dependence in the absence of taper, it would be surprising to find taper necessary in this model. The results (not shown) are indeed negative as expected; moderate degrees of forward taper at least, insufficient to necessitate $p_c(x)$-line tracking, do not cause negative $\mathrm{d}(p_1 - p_2)/\mathrm{d}Q$. The effect of forward taper (stiffer downstream) is to sharpen the knee in the flow rate limitation curves, relative to the case shown in Figure 4(c), while reverse taper produces a rounding of the knee.

4. DISCUSSION

The series of models explored here have interest primarily as an answer to the question: how basic can a collapsible-tube model be and still retain a given feature of observed collapsible-tube behaviour? In respect of the main qualitative aspects, it emerges that even a very simple model of the sort outlined here is adequate to predict or explain both pressure-drop limitation and flow rate limitation. This is a significant achievement, because some more sophisticated models have failed to do so. In particular, despite the inclusion of Bernoulli effects and the Borda-Carnot head loss that approximates flow separation at the end of the collapsed tube, in addition to viscous head loss varying with area, lumped-parameter models such as that of Bertram & Pedley (1982) failed to predict the appropriate shape of pressure-drop/flow rate curve when conditions for pressure-drop limitation were imposed. Specifically, that particular model predicted pressure-drop-limitation curves bending so that $\mathrm{d}(p_1 - p_2)/\mathrm{d}Q$ was greater than $(p_1 - p_2)/Q$; as noted earlier, this shape actually defines flow rate limitation. Bertram & Pedley (1982) concluded that distributed models were needed to overcome this problem. The simplest of the uniform-tube models examined here are lumped, in the sense that when the tube law is simply a switch from one value of resistance (or area) to another, the pressure profile consists of straight-line segments which are known once their end-points have been calculated. However, in one important respect the models are distributed: the position of collapse is variable. Thus, it is concluded that variable collapse position is the essential element missing from a lumped-parameter model which is needed to portray these behaviours correctly.

The pressure-drop/flow rate curves arising from the uniform-tube models also raise interesting questions about using the slope in region II (fixed p_e) to assess stability. Conrad, (1969), who introduced this idea, has tenaciously championed the criterion that self-excited oscillation arises only when the region-II slope is sufficiently negative that the overall system including up- and downstream parts has negative incremental resistance. While many observations have tended to support this criterion, there have also been reports of numerical (Matsuzaki & Seike 1996) and experimental (Ohba *et al.* 1989; Yamane & Orita 1992) oscillations occurring when the tube is in region III, suggesting that the criterion is not definitive. The models examined here are for steady flow only, and cannot say anything directly about stability. Nevertheless, the finding that the negative slope of region II can be abolished by reducing the resistance downstream of the collapsible tube is problematic for the Conrad criterion. A similar finding was made by Hayashi & Sato (1988), using a one-dimensional steady-flow model that included viscous resistance. Experimentally, it is well established (Bertram *et al.* 1990) that reducing downstream resistance promotes oscillatory instability. While the published data relate to values of downstream resistance considerably

greater than those examined here (relative to the resistance of the open collapsible tube), unpublished observations from this laboratory confirm that oscillations dominate when downstream resistance is almost completely abolished.

The model also has utility in understanding some of the range of behaviours available to a tube which varies in stiffness along its length, as do many if not all body conduits. It defines what degree of taper a tube must possess if required to behave functionally in one of the special ways which characterize forward-tapered tubes. It also provides the simplest possible tool with which to demonstrate the theoretical existence of these special configurations, and to understand the observed variability of throat position for such tubes during flow.

Has p_e-line tracking ever been observed experimentally? This may possibly be an explanation for the observation of Bertram & Chen (2000) that multiple throats form when a tapered-thickness tube is collapsed from the upstream end as far as an intermediate site. These successive minima of area are only just visible, i.e. considered as a standing wave, the amplitude is very weak, but up to four such minima have been seen. On this reading, these waves represent attempts to depart from the p_e-line on first one and then the other side. On the other hand, a completely different explanation is found in the idea of precursor waves (Kececioglu *et al.* 1981). Again it should be emphasized that tracking depends on the resistance of the collapsible tube switching between relatively fixed values, and is therefore largely an artefact of the extremely crude model explored here. The prediction of unattainable flow rates is more likely to be borne out experimentally, although again a more realistic tube law would probably convert the discontinuity in $Q(p_1)$ to a small range of p_1 values where flow rate changed rapidly.

Negative effort dependence, or a decrease in flow rate at around the knee representing the onset of flow rate limitation is apparently one phenomenon not comprehended by this model series, at least insofar as parameter space has been explored. The construction in Figure 6 showed clearly that one essential ingredient is a tube law allowing for more than one fixed value of collapsed resistance per unit length as in the simplest variety of this series. Yet exploration of tube laws giving finite or variable compliance when the tube is collapsed, and giving finite compliance when it is moving from first buckling to opposite wall contact, failed to produce negatively sloping pressure-drop/flow rate curves when upstream transmural pressure was held constant. Nor did reverse taper (stiffer upstream) or modest degrees of forward taper provoke such an effect. It remains to be seen whether this is a result of limited exploration of parameter space or whether the phenomenon requires inclusion of an aspect of collapsible tubes omitted here. Interestingly, the lumped-parameter model of Bertram & Pedley (1982) has no difficulty with negative effort dependence, since under conditions of constant upstream transmural pressure it displays hyperbolic pressure-drop/flow rate curves (unpublished calculations). However, as noted already, this model was unable to imitate pressure-drop limitation.

5. CONCLUSIONS

In conclusion, the most basic possible resistive model of a collapsible tube, together with more elaborate variations, has been examined. It was found that the most basic model showed realistic pressure drop/flow rate characteristics under all three important conditions: constant external pressure, constant downstream transmural pressure (pressure-drop limitation), and constant upstream transmural pressure (flow rate limitation). Comparison with a past lumped-parameter model showed that the essential element permitting this model to emulate these behaviours correctly was the movable collapse position. Endowing the model with finite collapsed compliance, with varying collapsed compliance, or with

finite compliance during collapse, although shown to be necessary, was not a sufficient condition to produce negative effort dependence. The Conrad criterion for oscillation onset was confirmed to be inapplicable when downstream resistance is small, suggesting a more general insufficiency.

Adapted to the situation of tubes with wall stiffness varying along their length, the model showed that qualitatively new behaviours arise only for the situation where the stiffness increases in the streamwise direction, and gave rise to a functional definition of an effectively tapered tube. Under the assumption of constant resistance per unit length both when open and when collapsed, six possible tube configurations were found, and ranges of unattainable flow rate were shown to exist when flow was propelled by a pressure head. Varying amounts of stiffness taper were shown to produce characteristic changes in the shape of the pressure-drop/flow rate relation at constant external pressure. Many of these findings are novel. Those that are not are nevertheless illuminating for being derived from so basic and comprehensible a model, which thus clearly shows which are the fundamental and essential aspects of a collapsible tube. The diagrammatic nature of the model gives it a particularly useful tutorial aspect.

References

Bertram, C. D. 1987 The effects of wall thickness, axial strain and end proximity on the pressure-area relation of collapsible tubes. *Journal of Biomechanics* **20,** 863–876.

Bertram, C. D. 1995 The dynamics of collapsible tubes. In *Biological Fluid Dynamics* (eds C. P. Ellington & T.J. Pedley), pp. 253–264. Cambridge, UK: Company of Biologists Ltd.

Bertram, C. D. & Chen, W. 2000 Flow limitation in a tapered-stiffness collapsible tube conveying a flow. *Journal of Fluids and Structures* (accepted).

Bertram, C.D. & Pedley, T.J. 1982 A mathematical model of unsteady collapsible tube behaviour. *Journal of Biomechanics* **15,** 39–50.

Bertram, C.D., Raymond, C.J. & Pedley, T.J. 1990 Mapping of instabilities for flow through collapsed tubes of differing length. *Journal of Fluids and Structures* **4,** 125–153.

Conrad, W. A. 1969 Pressure-flow relationships in collapsible tubes. *IEEE Transactions on Bio-Medical Engineering* **16,** 284–295.

Conrad, W. A. 1995 Discussion: relationship of pressure wave velocity to self-excited oscillation of collapsible tube flow. *JSME International Journal Series A* **38,** 138.

Elad, D., Sahar, M., Avidor, J.M. & Einav, S. 1992 Steady flow through collapsible tubes: measurements of flow and geometry. *ASME Journal of Biomechanical Engineering* **114,** 84–91.

Fry, D.L., Thomas, L.J. & Greenfield, J.C. 1980 Flow in collapsible tubes. In *Basic Hemodynamics and its Role in Disease Processes* (eds D. J. Patel & R. N. Vaishnav), pp. 407–424. Baltimore, MD: University Park Press.

Griffiths, D. J. 1975 Negative-resistance effects in flow through collapsible tubes. *Medical and Biological Engineering* **13,** 785–802.

Hayashi, S., Honda, T. & Tanba, M. 1994 Stability of steady flow in collapsible tubes. *JSME International Journal Series B* **37,** 349–354.

Hayashi, S. & Sato, K. 1988 Static characteristics of collapsible tubes. *Proceedings of the Second International Symposium on Fluid Control, Measurement, Mechanics & Flow Visualisation* (ed. R. F. Boucher), pp. 234–238, Sheffield, U.K.

Heil, M. & Pedley, T. J. 1996 Large post-buckling deformations of cylindrical shells conveying viscous flow. *Journal of Fluids and Structures* **10,** 565–599.

Jensen, O. E. 1998 An asymptotic model of viscous flow limitation in a highly collapsed channel. *ASME Journal of Biomechanical Engineering* **120,** 544–546.

Kamm, R. D., Elad, D., Jaekle, D. E. jr. & Shapiro, A.H. 1991 Theory and experiments on smooth transitions through the critical state ($S = 1$) in collapsible tube flow. In *1991 Advances in Bioengineering* (ed. R. Vanderby Jr.), ASME BED-Vol. 20, pp. 329–332. New York: ASME.

Kamm, R. D., Patel, N. R. & Elad, D. 1993 On the effect of flow-induced flutter on flow rate during a forced vital capacity maneuver. *FASEB Journal* **7,** A11.

Kececioglu, I., McClurken, M. E., Kamm, R. D. & Shapiro, A. H. 1981 Steady, supercritical flow in collapsible tubes. Part 1. Experimental observations. *Journal of Fluid Mechanics* **109,** 367–389.

Matsuzaki, Y. & Seike, K. 1996 Numerical analysis of flow in a collapsible vessel based on unsteady and quasi-steady flow theories. In *Computational Biomechanics* (eds K. Hayashi & H. Ishikawa), pp. 185–198. Tokyo: Springer-Verlag.

Mead, J., Turner, J. M., Macklem, P. T. & Little, J. B. 1967 Significance of the relationship between lung recoil and maximum expiratory flow. *Journal of Applied Physiology* **22,** 95–108.

Ohba, K., Aono, M., Yoneyama, N. & Sakurai, A. 1989 Flow oscillation and wave propagation in collapsible tube. In *Progress and New Directions of Biomechanics* (eds Y. C. Fung *et al.*), pp. 213-227. Tokyo: Mita Press.

Ohba, K., Sakurai, A. & Maekawa, K. 1998 Characteristics of the flow in collapsible tube with continuously varying compliance along the tube axis—its application to extracorporeal circulation. *Abstracts of the Third World Congress of Biomechanics*, Sapporo, Japan, 2–8 Aug. (eds Y. Matsuzaki *et al.*), p. 38.

Shapiro, A. H. 1977 Steady flow in collapsible tubes. *ASME Journal of Biomechanical Engineering* **99,** 126–147.

Wilson, T. A., Rodarte, J. R. & Butler, J. P. 1986 Wave-speed and viscous flow limitation. In *Handbook of Physiology*, Section 3, Vol. III, pp. 55–61. Bethesda, MD: American Physiological Society.

Yamane, T. & Orita, T. 1992 Self-excited oscillations with and without supercritical flow in collapsible tubes. *Proceedings of the Seventh International Conference on Biomedical Engineering*, Singapore, 2–4, Dec. pp. 502–504.

Yamane, T. & Orita, T. 1994 Relationship of pressure wave velocity to self-excited oscillation of collapsible tube flow. *JSME International Journal Series A* **37,** 71–78. Discussion: *JSME International Journal Series A* **38,** 138–140 (1995).